INTERACTION OF A NEUTRAL CLOUD MOVING THROUGH A MAGNETIZED PLASMA

C. K. Goertz and G. Lu

Department of Physics and Astronomy, University of Iowa, Iowa City

Abstract. Current collection by outgassing probes in motion relative to a magnetized plasma may be significantly affected by plasma processes that cause electron heating and cross field transport. Simulations of a neutral gas cloud moving across a static magnetic field are discussed. We treat a low-β plasma and use a $2-1/2$ D electrostatic code linked with our Plasma and Neutral Interaction Code (PANIC). Our study emphasizes the understanding of the interface between the neutral gas cloud and the surrounding plasma where electrons are heated and can diffuse across field lines. When ionization or charge exchange collisions occur a sheath-like structure is formed at the surface of the neutral gas. In that region the crossfield component of the electric field causes the electron to $\vec{E} \times \vec{B}$ drift with a velocity of the order of the neutral gas velocity times the square root of the ion to electron mass ratio. In addition a diamagnetic drift of the electron occurs due to the number density and temperature inhomogeneity in the front. These drift currents excite the lower- hybrid waves with the wave k-vectors almost perpendicular to the neutral flow and magnetic field again resulting in electron heating. The thermal electron current is significantly enhanced due to this heating.

1. Introduction

It is well known that a neutral gas moving across a magnetic field relative to a plasma causes plasma heating [Machida and Goertz, 1988] and if the relative speed exceeds the Critical Ionization Velocity (CIV) V_c the neutral gas can be rapidly ionized. [see e.g. Brenning, 1981]. This anomously rapid ionization phenomenon was first discussed by Alfvén [1954] who postulated that CIV occurs when the kinetic energy of the neutral particles ($m_n V_c^2/2$) exceeds the ionization energy ($e\phi_{ion}$) of the neutrals. Although CIV is not directly relevant to current collection in space the microscopic process that leads to electron heating is because it enhances the electron current that can be collected. Turbulence may also allow for rapid transport across magnetic field lines.

The electron heating proceeds in two steps. First the neutrals give energy to ions and then the ions energize the electrons. The energy transfer from neutrals to ions involves the charging of a neutral either by charge exchange or ionization; the transfer of energy from ions to electrons involves the excitation of plasma waves by the moving ions and their subsequent damping by electrons [Raadu, 1978; Galeev, 1981; Abe, 1984; Abe and Machida, 1985; Papdopoulous 1985; Machida and Goertz, 1987]. There is also a more direct way for energizing the electrons. This process occurs in the leading edge of the neutral gas as it moves through the plasma and works in the following manner. If a moving neutral is charged by photoionization, impact ionization or charge exchange the newly created ion will continue to move across the magnetic field with the neutral particle's speed. The plasma electrons are tied to the magnetic field and remain at rest. Thus a charge separation occurs at the edge of the neutral cloud and an electric field pointing into the neutral cloud develops. This electric field causes a secondary electron drift along the front of the neutral gas cloud. Ions are very massive and will not drift in response to this spatially limited field. The electron drift speed can be large and destabilize lower hybrid electrostatic waves by the modified two- stream instability which in turn heat the electrons. Thus intense waves should exist in this front. If the electron energy becomes large enough impact ionization by the energetic electrons creates new ion-electron pairs thus providing a positive feedback process. Whereas the waves and electron heating inside the neutral cloud has been studied extensively before very little theoretical work has been done on the structure and dynamics of the front. In this paper we report the results of a 2 - 1/2 D electrostatic code linked with our Plasma and Neutral Interaction Code (PANIC, see Machida and Goertz, 1987) which focuses on the understanding of this front.

Plasma turbulence inside a neutral gas moving through a magnetized plasma may affect current collection by outgassing probes in two ways. The increased electron temperature increases the thermal electron current. In addition, turbulence can cause enhanced diffusive transport of electrons across magnetic field lines and thus lead to an increased effective collecting area of a probe. This enhanced diffusion has been discussed by Sudan (1983, a, b) and has been verified by simulations (Machida and Goertz, 1988).

2. The Charge Separation

Consider a moving neutral at the interface between a neutral cloud and a plasma that is charged (either by a UV photon or an energetic electron or by charge exchange with a stationary ion). Electrons are trapped by the magnetic field pointing out of the plane of figure 1. The ion moves into the plasma at the speed of the neutral. A charge separation evolves and a potential jump occurs at the plasma - neutral gas interface. Clearly the potential will not greatly exceed a value necessary to reflect the ion. Thus

$$e\phi \sim m_i V_n^2/2 \tag{1}$$

The distance, D, over which a finite electric field exists is difficult to estimate. It is clearly smaller than an ion-gyroradius and larger than an electron - gyroradius. An exact theory for D is difficult because the charge separation may be effected by the pre-existing background plasma outside the neutral cloud. For example plasma ions moving to the left in figure 1 can be accelerated through the potential and plasma electrons could be trapped within the front. It seems reasonable to assume that D is of the order of the hybrid gyroradius

$$D = \sqrt{R_e R_i} \tag{2}$$

where the newly created particle's gyroradius is

$$R_j = \frac{V_n}{q_j B_0} m_j \quad ; \quad j = e,\ i \tag{3}$$

Thus the electric field $E = \phi/D$ will cause all electrons within the front to drift (upwards in figure 1) at a speed

$$V_D = \frac{E}{B_0} = \frac{V_n}{2}\sqrt{\frac{m_i}{m_e}} \tag{4}$$

The drift energy of these electrons is

$$K = \frac{m_e}{2} V_D^2 = \frac{1}{4}\left[\frac{m_i V_n^2}{2}\right] \tag{5}$$

If a probe would be inserted into this front one would expect an enhanced electron current because K can be larger than the electron thermal energy. However, it is not clear that the estimate of D given above is correct.

Because the electron drift speed is large only inside this charge separation front one expects an electron pressure enhancement there. In that case one must consider the electron density gradient drift:

$$V_g = \frac{1}{n_e B_0} \nabla (n_e T_e) \tag{6}$$

Using the scale length D to represent the pressure gradient by $n_e T_e / D$ we find that

$$\frac{V_g}{V_D} = \frac{m_e}{m_i} \frac{V_e}{V_n} \tag{7}$$

where V_e is the electron thermal velocity. If the electrons will be thermalized with $V_e = \sqrt{m_i/m_e} V_n$ we find that $V_g/V_D = O(\sqrt{m_e/m_i})$. Thus one may presume that the diamagnetic drift is unimportant. However, the plasma waves excited depend on the magnitude of this drift even when it is small.

Using a local approximation for electrostatic waves propagating in a plane the dispersion relation is given by

$$1 + (\frac{\omega_{pi}}{kV_i})^2 (1 + \varsigma_i Z(\varsigma_i)) + (\frac{\omega_{pe}}{kV_e})^2 (1 + I_0(b) e^{-b} (1 - \frac{\omega_2}{\omega_1}) \varsigma_e Z(\varsigma_e)) = 0$$

$$\varsigma_i = \omega / \sqrt{2} k V_i$$

$$\varsigma_e = (\omega - k_\perp V_D) / \sqrt{2} k_\parallel V_e \tag{8}$$

$$b = (k_\perp V_e / \Omega_e)^2$$

$$\omega_1 = \omega - k_\perp V_D$$

$$\omega_2 = k_\perp V_g$$

[Gladd, 1976].

For $| \omega_2/\omega_1 | = 0$ waves are excited by the modified two- stream instability with

$$\omega_r \sim (\sqrt{3}/2) \omega_{LH}$$

$$\gamma_{max} \sim \omega_{LH}/2 \tag{9}$$

The waves propagate not exactly perpendicular to B_0 but grow most rapidly for

$$k_{\parallel}/k \sim \sqrt{m_e/m_i} \tag{10}$$

Because of this they have an electric field component along the magnetic field which causes electron Landau damping and hence electron heating.

On the other hand, if $\mid \omega_2/\omega_1 \mid$ is not very much smaller than 1 the lower - hybrid drift instability is generated with:

$$\omega_r \sim \omega_{LH}$$

$$\gamma_{max} \sim \omega_{LH}$$

This mode propagating exactly perpendicular to B_0 (i.e. $k_{\parallel}/k = 0$) would not suffer electron Landau damping and hence not lead to parallel electron heating. It may, however, give rise to an enhanced effective collision frequency which allows electrons to move across B and along the background electric field and hence to gain energy (Machida and Goertz, 1988).

Figure 2 shows an exact solution of the dispersion relation (8) for parameters relevant to the simulation runs described later ($m_i/m_e = 100$). If the gradient drift velocity had been neglected the growth rate would approach zero for $k_{\parallel}/k \rightarrow 0$. The waves with $k_{\parallel}/k \geq 0.1$ are due to the modified two stream instability and for $k_{\parallel}/k \leq 0.1$ they are mainly due to the lower hybrid drift instability. This linear theory does, of course, not predict the non-linearly saturated wave spectrum and is thus not capable of making predictions about the electron temperature in the neutral gas cloud and its front. One may, for example, expect that as the modified two-stream instability excited by V_D saturates by electron trapping and heating. The pressure gradient drift V_g grows and the wave energy shifts to smaller values of $k_{\parallel}/k$ reducing the electron heating efficiency in the front. Clearly, only a numerical simulation will allow us to investigate this.

3. Simulation

The electrostatic PIC simulation code used for this work has been described in a previous paper (Machida and Goertz, 1987). It has been used to investigate the CIV process in homogeneous gas

clouds (Machida and Goertz, 1987) and in finite size clouds with special emphasis on the ionization front by Machida et al. (1988). We have also used it to investigate the anomalous heating of electrons that occurs when an electric field is applied perpendicular to a magnetic field (Machida and Goertz, 1988). In that work the relative drift between plasma and neutrals was below the critical velocity. It is most closely related to the work reported here. In this work, however, we deal with a finite size cloud whereas in Machida and Goertz (1988) the neutral gas density was assumed to be homogeneous. In this paper we include the following collisional processes as in Machida and Goertz (1988):

a. Elastic electron-neutral and ion-neutral collisions (collision frequency ν_{en}, ν_{in})

b. Inelastic electron-neutral collisions. In these collisions the electrons lose a certain amount of energy to the excitation of neutrals. The collision frequency is ν_e^* and the threshold energy is E^*. In each collision the electron loses an energy equal to E^*.

c. Charge exchange collisions between ions and neutrals occur at a collision frequency ν_{chx}.

d. Electron ionizing collisions ν_{ion} occur only if the electron energy is above the ionization threshold energy $e\phi_{ion}$. Since the relative drift between plasma and neutrals is smaller than the critical velocity v_c few ionizing collisions occur.

The values used in the simulation for these parameters are given in Table 1. Since resistive heating is proportional to V_D^2 and the collisional cooling is proportional to E^* these values would indicate that without wave heating the electrons would rapidly cool inside the neutral cloud. And, indeed, when we run our code without the Poisson solver (i.e. no self- consistently generated waves present) the electrons inside the neutral gas cool as expected (data not shown).

The relative drift $\vec{V}_D$, between plasma and neutrals is implemented by applying a constant electric field $\vec{E}_o = \vec{B}_o \times \vec{V}_D$ to the simulation. The perturbation field $\vec{E}'$ of the waves and in the charge separation front is calculated self-consistently from Poisson's equation.

We have used two shapes for the neutral gas cloud. In the first set of runs we have used a neutral gas slab as shown in Figure 3a. This shape is unrealistic but allows for easier comparison

with theory. In the second set of runs we have used a circular gas cloud as shown in Figure 3b. A control run was also made with no collisions included (all ν were set equal to zero) which corresponds to a zero neutral gas density. The diagnostics include calculations of density, electrostatic fields $\vec{E}'$ and potentials Φ', electron and ion temperatures, phase space plots and a calculation of the thermal electron flux penetrating a certain small area in the simulation region. In addition we can determine the frequency and wave- number spectra of the electric field fluctuations. A detailed description of all our results using the full set of diagnostics will be published elsewhere.

4. Results

In this paper we are mainly interested in the electron heating that occurs due to collisions and wave-particle interactions. In Machida and Goertz (1988) we found that after a few 100 ω_{pe}^{-1} the electron temperature saturated at a value given by

$$kT_e = \eta m_i V_D^2/2$$

The value of η varied from 0.2 to 0.7 depending on whether lower hybrid wave heating was allowed to occur in the simulation or not. At the shuttle orbit altitudes $m_i V_D^2/2$ may be as large as 3eV. Thus this heating could be quite significant. It is the purpose of this work to find out whether the value of η is significantly affected by using a finite size cloud.

4.1. Control Run

A control run was made with all collision frequencies set to zero. This run shows the effects of inherent numerical heating and noise in the code. Figure 4a shows the evolution of T_e with time. Little numerical heating occurred. The temperature increased only by 5%. The electrostatic field frequency spectrum is shown in figures 4b and 4c at different times during the run. The noise level is reasonably small. A small enhancement near the lower and upper hybrid frequency can be seen. The electrostatic potential contours are shown in Figure 4d. No large potentials occur. This run together with the collisional run without the Poisson solver implemented which displayed electron

cooling suggests that any electron heating observed in the subsequent runs is due to wave-particle interactions.

4.2. Neutral Gas Slab Model

Figure 5a shows the evolution of the electron thermal energy (drift energy is subtracted) averaged over the volume occupied by the neutral clouds. In this run the magnetic field is perpendicular to the plane ($\vec{B} = B_o\hat{z}$). Heating in the cloud is quite obvious. The electron temperature saturates at $kT_e = \eta m_i V_D^2/2$ with $\eta = 1.1$. Figure 5b and 5c show the electrostatic field spectra at different times. These spectra were obtained in the center of the simulation region (indicated by a cross in Figure 3a). The low frequency peak is at the lower hybrid frequency. The high frequency noise is centered around the upper hybrid frequency. Figure 5d shows equipotential contours. Comparing this with Figure 4d reveals that large electric fields in the direction of the plasma motion (from right to left) are produced as expected and discussed in Section 2. The total potential drop between the leading and trailing edge of the cloud indicated by the dashed lines is about $10kT_eo$ or 0.8 mV_D^2.

In Figure 5 the magnetic field was assumed to be perpendicular to the simulation plane $\vec{B} = B_o\hat{z}$. Since lower hybrid waves created by the modified two stream instability have a finite $k_{||}$ they cannot be excited in this configuration. (See also discussion in Machida and Goertz, 1986.) Thus the electron heating must be mainly due to enhanced resistive heating (enhanced effective collision frequency) and heating by waves driven by the gradient drift instability with $k_{||} = 0$. In addition in this run the secondary $\vec{E} \times \vec{B}$ drift due to the charge separation field is in the plane of the simulation (in the $-\hat{y}$ direction). Elastic scattering of electrons may transform part of that drift energy into thermal energy.

To allow for the presence of lower hybrid waves driven by the ion beams created by charge exchange we have made another run in which the magnetic field was in the plane of the simulation ($\vec{B} = B_{oy}\hat{y}$). The applied electric field is given by $\vec{E}_o = \vec{B} \times \vec{V}_D$ where $\vec{V}_D = -V_D\hat{x}$. In this case lower hybrid waves driven by the ion beams can be generated. Figure 6 shows the same diagnostics as before.

Surprisingly the electron temperature increase is slightly smaller ($\eta \rightarrow 1.0$) but the fluctuation power spectrum more intense than in the previous case. In this case the gradient drift instability cannot be excited because it must propagate in the y - z plane and our two-dimensional simulation has k_z (equal to $k_\perp$ in this case) equal to zero.

4.3. Circular Gas Cloud Model

One may expect that lower hybrid waves could not be excited if the neutral gas cloud is smaller than the wavelength of the excited waves. In the previous case the cloud is infinite in the $\hat{y}$ direction (periodic boundary conditions in $\hat{y}$). In the circular cloud model the cloud is of finite size. One may also suspect that heated electrons will escape from the cloud and be replaced by cold electrons from the surrounding plasma. Thus we expected that the electron temperature increase would not be as large in this case as in the slab model case.

Figure 7 shows that this is, indeed, the case. Figure 7 shows the results for $\vec{B} = B_{oy}\hat{y}$,. We see that the charge separation field is only slightly affected by the cloud's finite size. The temperature increase is not as rapid as before but the temperature has not saturated by the end of the run and it is not clear that the final saturated T_e will be different from the previous case. When a normal magnetic field ($B_{oz} \gg B_{oy}$) is added the escape of electrons from the cloud is reduced and the temperature increase is faster, almost comparable to the slab model case (data not shown). We have not analyzed this case in detail and plan to report on more detailed diagnostics in a future paper.

4.4. Electron Thermal Current

As a first step towards understanding how these results affect the current that can be collected from a probe placed inside a neutral cloud penetrated by a magnetized plasma flow we have calculated the number of electrons hitting a flat plate placed inside the neutral cloud between t = 0 and t divided by the time t as a function of time t. We have used two orientations for the plate. In the first case the plate is placed parallel to the plasma flow. The plate's normal is in the $\hat{y}$ direction. In this case electrons streaming parallel to the magnetic field B_{oy} are intercepted by the plate. The plate is 5

grid spaces wide. In the second case the plate is placed perpendicular to the flow with its normal pointing in the $\hat{x}$ direction (see Figure 3b). In this case the plate intercepts electrons which have a velocity component perpendicular to the magnetic field.

The results are shown in Figure 8a for the perpendicular orientation and in Figure 8b for the parallel orientation. Five curves are shown in each case. The solid line is the control run and shows a low almost contant electron flux, the dashed lines are for the slab model and the dotted lines are for the circular cloud model. The double dashed line is for $\vec{B} = B_{oz}\hat{z}$. The large dots are also for $\vec{B} = B_{oz}\hat{z}$. The singly dashed line and the small dots are for $\vec{B} = B_{oy}\hat{y}$. The increase of the electron flux due to the neutral gas driven heating processes is quite obvious for the slab model. The fact that the integrated currents evolve different for the two different orientations of the plate indicates that the electron heating is anisotropic. The current collected inside a circular cloud is not vastly different from the control run which we attribute to escape of electrons from the cloud. These results are, of course, quite preliminary and require more detailed diagnostics. The difference between the slab and circular model cases may also be affected by the fact that in the circular cloud model the center of the cloud where the plate was placed was positively charged and thus may have contained low density electron beams.

5. Discussion

As expected the leading edge of a neutral cloud becomes positively charged and an electric field pointing in the direction of the plasma flow occurs. The total potential drop across the neutral cloud can reach values several times $m_i V_D^2/2e$. This charge separation electric field causes a rapid $\vec{E} \times \vec{B}$ drift of the electrons. This drift appears to be fast enough to destabilize the modified two stream instability which can cause strong electron heating. We have found previously that this source for wave generation is more important than the more direct source of ion beams created by charge exchange or ionization (Machida et al., 1988). We also find that the gradient drift instability is important.

We have not found that the waves are suppressed in a small neutral cloud even if the cloud

is smaller than the wavelength of the most unstable waves (roughly the hybrid gyroradius $R_H = \sqrt{R_i R_e}$). The escape of hot electrons from the neutral cloud does slow the heating rate but is not such an efficient cooling mechanism that the heating is suppressed. The heating of electrons does appear to be anisotropic.

Due to the heating of electrons the thermal electron flux is enhanced which should allow for enhanced current colleciton. This result must, however, be considered as tentative because we have not yet included the charging of a probe to the floating potential. In that case we expect the particle orbits to be significantly different and the current collected may differ considerably from the values indicated by our preliminary results. The position of a probe relative to the edge of the cloud may also be an important factor which we have not studied. We also intend to investigate in a later work the effects of a bias voltage on a probe placed inside the neutral cloud.

This work is also incomplete in the following sense. Whereas these simulations can be used to illustrate the basic physical principles they cannot make quantitative predictions to be used for applications to current collection in space. This is due to computational limitations. For example the mass ratio $m_i/m_e = 100$ is totally unrealistic. The simulation region is only a few hundred Debye lengths wide which is much smaller than any real outgassing cloud. The collision frequencies are artificially high. If we were to reduce ν/ω_{pe} to realistic values the run time would have to be several orders of magnitude larger. These shortcomings are, of course, not unique to our simulation. They will plague simulations for a long time to come. This does not, however, mean that simulations are useless. Their values lies in their ability to isolate physical processes, assess their relative importance and derive scaling laws from a comparison with analytic theory. We have not yet accomplished this for the runs described here.

Acknowledgements. The authors would like to thank T. Whelan for his help with code modifications. This work was in part supported by NASA Grant NSG-7632, NSF Grant ATM-8411311, and the Lockheed Company.

Parameters

	Control Run	Neutral Cloud	Comments
m_i/m_e	100	100	
v_D/v_{eo}	0.24	0.24	initial ion thermal velocity v_{eo}
ω_{pe}/Ω_e	1	1	
ν_{ee}/ω_{pe}	0	0.02	electron-neutral elastic collision
ν_{ie}/ω_{pe}	0	0.02	ion-neutral elastic collision
ν_e^*/ω_{pe}	0	0.02	electron-neutral inelastic collision
E^*/kT_{eo}	1.8	1.8	threshold energy for inelastic collis
ν_{chx}/ω_{pe}	0	0.04	charge exchange
ν_{ion}/ω_{pe}	0	0.04	ionization
$e\phi_{ion}/kT_{eo}$	7.3	7.3	ionization energy

References

Abe, T., Theory of the critical ionization velocity phenomenon, Planet. Space Sci., 32, 903-906, 1984.

Abe, T., and S. Machida, Production of high-energy electrons caused by counterstreaming ion beams in an external magnetic field, Phys. Fluids, 28, 1178-1185, 1985.

Alfvén, H., On the origin of the solar system, Oxford University Press, New York, 1954.

Brenning, N., Experiments on the critical ionization velocity interaction in weak magnetic field, Plasma Phys., 23, 967 -, 1978.

Galeev, A. A., Proceedings of the International Schools and Workshop on Plasma Astrophysics, Varenna, Eur. Space Agency Spec. Publ., SP-161, 77-82, 1981.

Gladd, N. T., The lower hybrid drift instability and the modified two stream instability in high density theta pinch environments, Plasma Phys., 18, 27-40, 1976.

Machida S. and C. K. Goertz, Computer simulation of the Farley-Buneman instability and anomalous electron heating in the auroral ionosphere, J. Geophys. Res., 93, 9993-10,000, 1988.

Machida, S., and C. K. Goertz, A simulation study of the critical ionization velocity process, J. Geophys. Res., 91, 11965-11976, 1986.

Machida, S., and C. K. Goertz, The electromagnetic effect on the critical ionization velocity process, J. Geophys. Res., *aunderline*93, 11,495-11,506, 1988.

Machida, S., C. K. Goertz and G. Lu, Simulation study of the ionizing front in the critical ionization velocity phenomenon, J. Geomag. Geoelectr., 40, 1205-1219, 1980.

Papadopoulous, K., On the physics of the critical ionization velocity phenomena, in Advances in Space Plasma Physics, edited by B. Buti, p33-58, World Scientific Publication Company, Singapore, 1985.

Raadu, M. A., The role of electrostatic instabilities in the critical ionization velocity mechanism, Astrophys. Space Sci., 55, 125-138, 1978.

Sudan, R. N., Nonlinear theory of type I irregularities in the equatorial electroject, Geophys. Res. Lett., 10, 983, 1983a.

Sudan, R. N., Unified theory of type I and type II irregularities in the equatorial electroject, J. Geophys. Res., 88, 4853, 1983a.

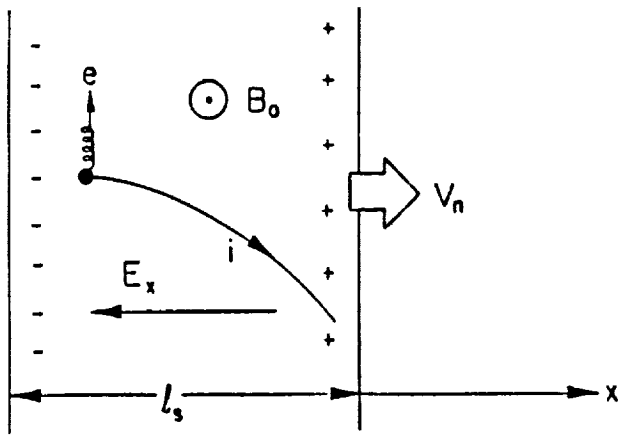

Figure 1. Schematic illustration of the charge separation front. Note that this figure is in the rest frame of the plasma. The neutral gas moves to the right.

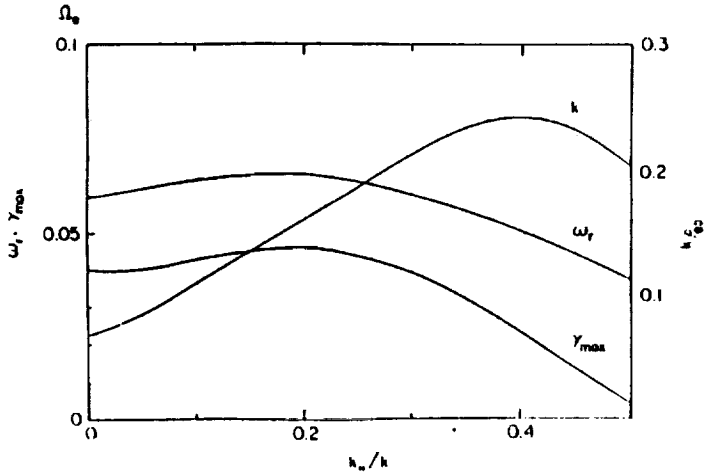

Figure 2. The maximum linear growth rate γ_{max}, corresponding to the real wave frequence ω_r and wave number k plotted as a function of $k_\parallel/k$.

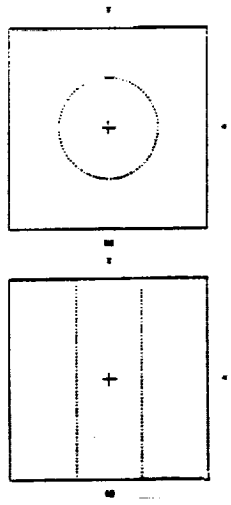

Figure 3. The geometry of the simulations for the slab model (a) and circular cloud model (b). The magnetic field can have either a $\hat{y}$ or $\hat{z}$ component or both. The plasma drifts from right to left in both cases.

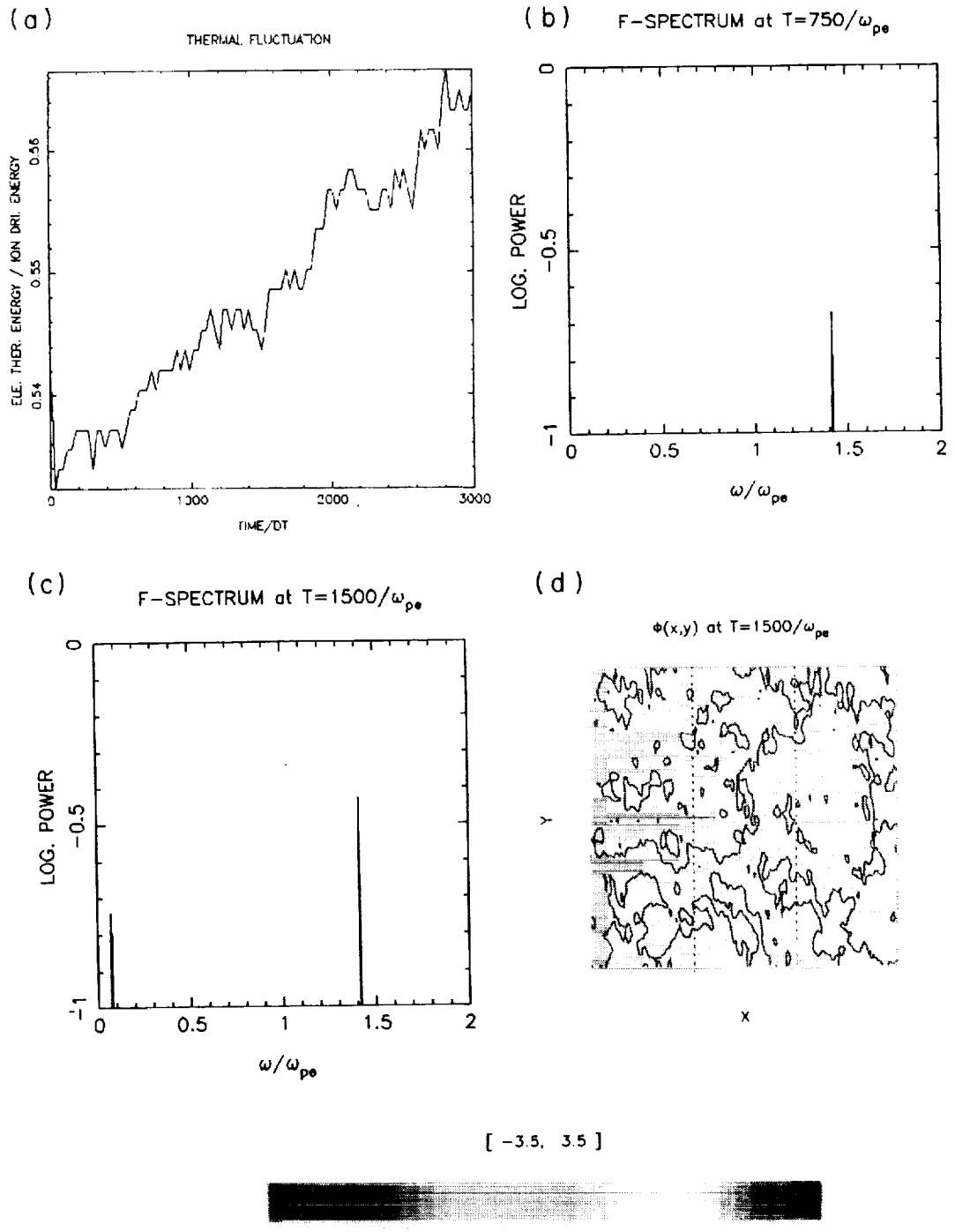

Figure 4. The time evolution of the total electron thermal energy ($\frac{3}{2}kT_e$) normalized to the ion drift energy ($m_iV_D^2/2$) (a). The power spectra at $t = 750\omega_{pe}^{-1}$ (b) and $t = 1500\omega_{pe}^{-1}$ (c) taken in the center of the simulation region. The equipotential contours (d) in units of kT_{eo}/e where T_{eo} is the initial electron temperature.

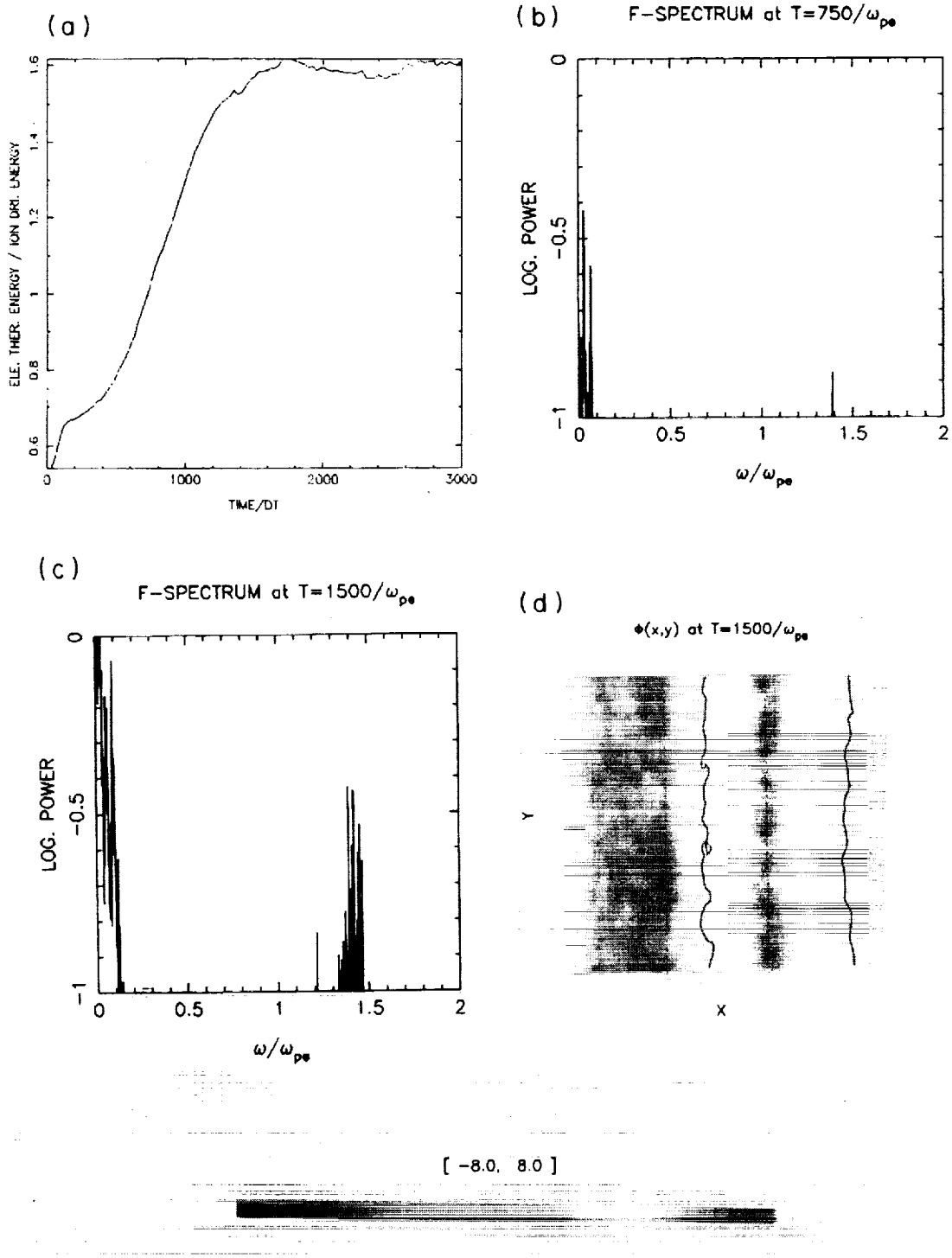

Figure 5. Same as Figure 4 for the slab model. The magnetic field is $\vec{B} = B_{os}\hat{z}$.

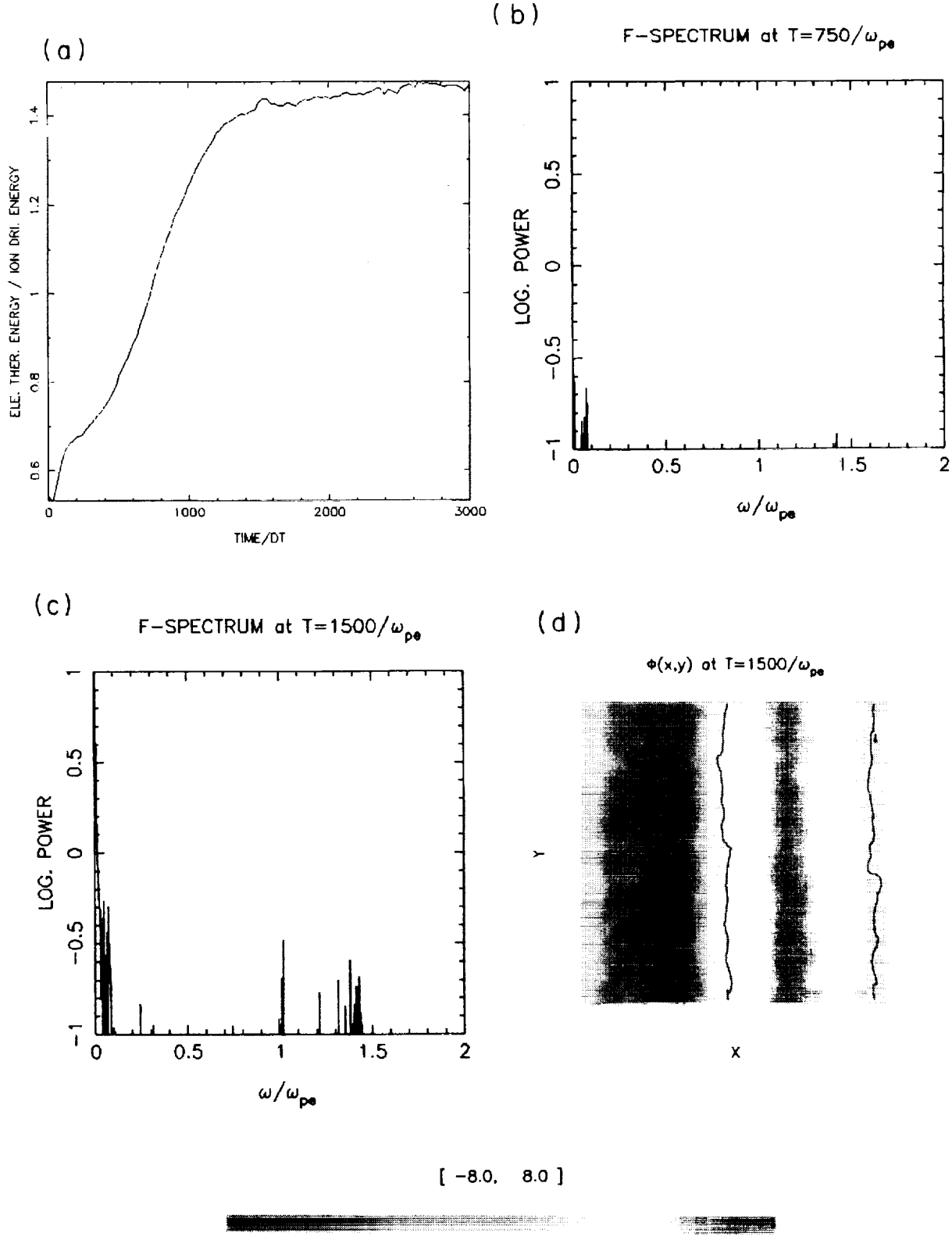

Figure 6. Same as Figure 5 except that in this case $\vec{B} = B_{oy}\hat{y}$.

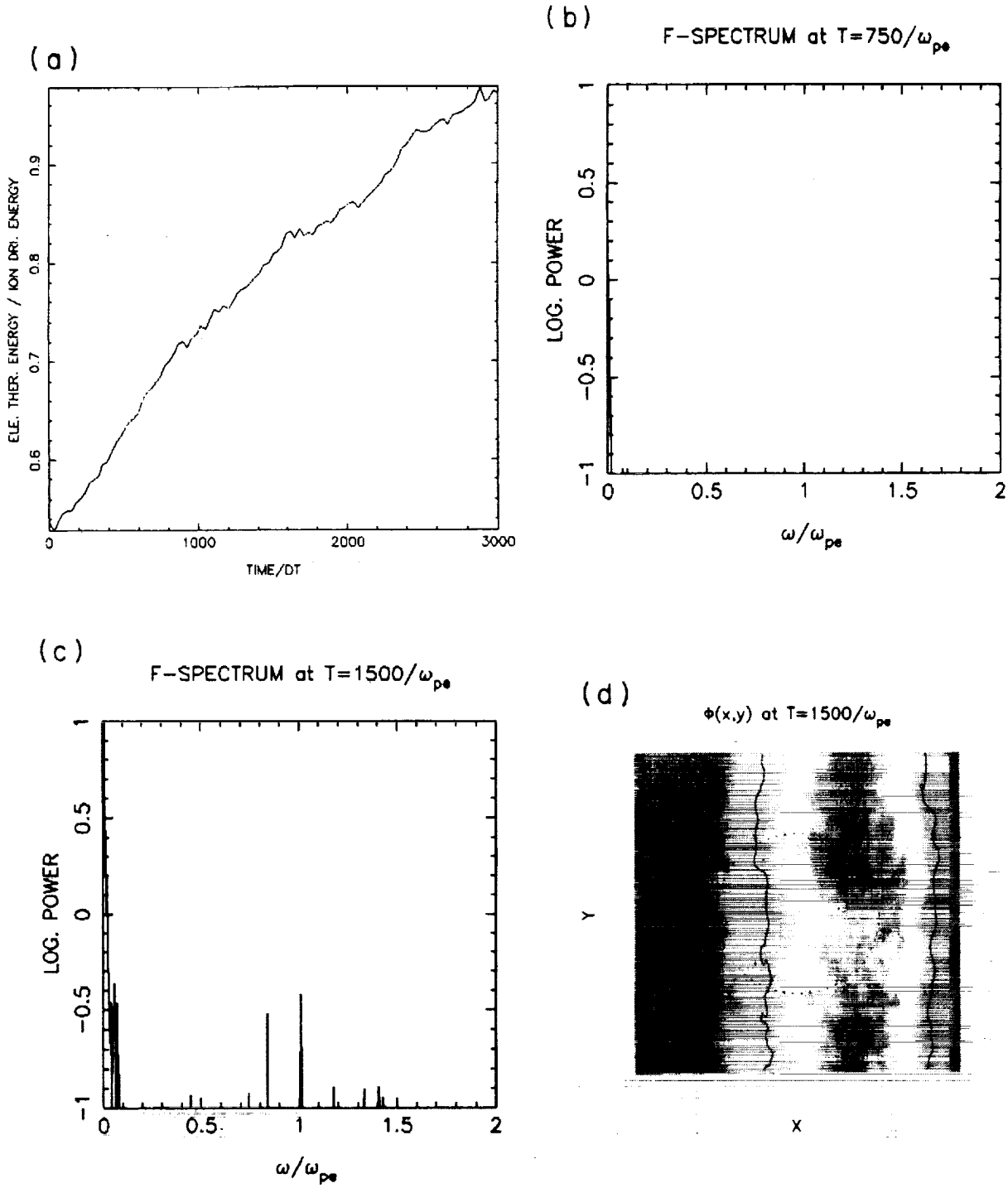

Figure 7. Same as Figure 6 for the circular cloud model.

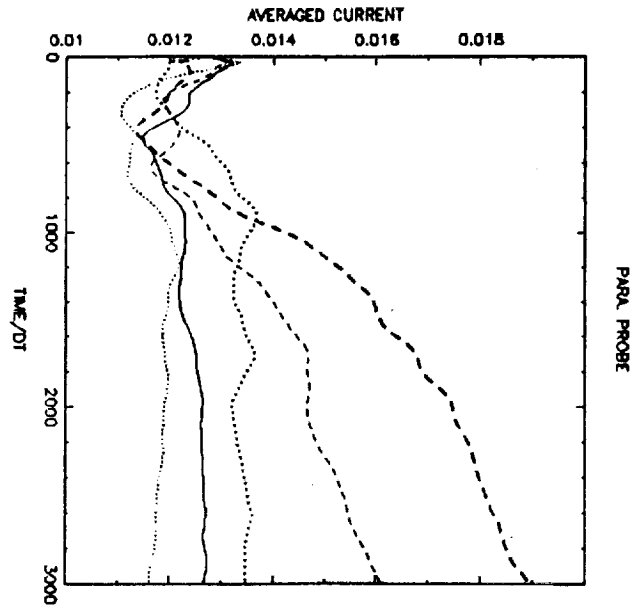

Figure 8a.

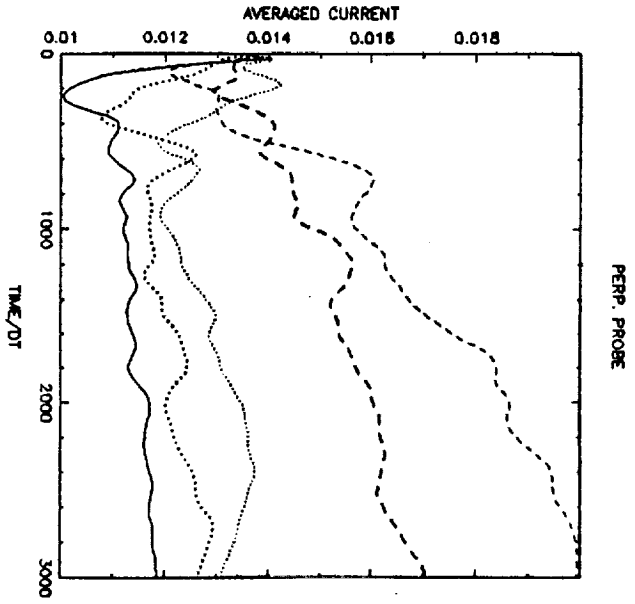

Figure 8b.

Figure 8.

(a) The rate of electrons absorbed by a flat plate oriented parallel to the flow (plate normal parallel to $\hat{y}$).

(b) The rate of electrons absorbed by a flat plate oriented perpendicular to the flow (normal parallel to $\hat{x}$). The solid line is from the control run (figure 4); the dashed lines are from the slab (figures 5 and 6) and the dotted lines from the circular cloud (figure 7).